Evaluating the Effects of Switching Period of Communication Topologies and Delays on Electric Connected Vehicles Stream with Car-following Theory

Hang Zhao, Yongfu Li, *Member, IEEE*, Wei Hao, Srinivas Peeta, Yibing Wang, *Member, IEEE*

***Abstract*—Unstable vehicle-to-vehicle (V2V) communication connections are a vital phenomenon in connected vehicle (CV) environments which lead to the change of communication topologies and delays among electric connected vehicles (ECVs). This paper aims to evaluate the effects of the switching period of communication topology and delay on the dynamic performance and energy consumption of an ECV traffic stream considering the characteristics of car-following (CF) theory. To this end, a communication topology characterization method is developed by using the beacon transmission mechanism, graph theory, and probability theory. Then, a new CF model incorporating the effects of the communication topologies and delays is proposed to capture the interactions under a CV environment. The stability of the proposed model is analyzed by using the perturbation method. Finally, extensive simulations are implemented to be separately discussed by considering the effects of different switching periods of communication topologies and delays.**

***Index Terms*—Electric connected vehicle, Car-following model, Communication topology, Communication delay, Energy consumption**

I. Introduction

Energy consumption (EC) is one of the main concerns in transportation systems [1-3]. So far, two aspects of major researches are underway to seek an optimal energy-efficient scheme. One of which is from the viewpoint of transportation system. In other words, connected vehicle (CV) technology originated from wireless communication and sensing technology is developed to coordinate the space and time resources of transportation system under energy consumption (EC) constraints [4-11]. Consequently, this objective drives the research of car-following (CF) theory in depth. Because CF model is viewed as an effective tool to reproduce the characteristics of traffic stream and evaluate its EC as well [12]. On the other hand, in the automotive manufacturing field, researchers and engineers devote to developing electric vehicle (EV) technology as EVs can travel by utilizing renewable energy instead of oil and gas [13].

The recent developments of CV technology promote the research of CF behavior studies. In particular, many CF models and their variants have been proposed to enhance dynamic performance by incorporating various factors, such as the stimuli (i.e., headway, velocity and acceleration difference) from multiple preceding vehicles [14, 15], vehicle dynamics (i.e., electronic throttle opening angle) [16], gap distribution (i.e., lateral gap) and road geometry (i.e., gradient and curvature) [17-20].

However, most of these CF models study the traffic stream with the assumption that all vehicles travel in a traffic environment with full information. Meanwhile, the information of all vehicles in that traffic stream can be successfully obtained by the objective vehicle. Hence, it is hard to directly utilize them in evaluating the dynamic performance and EC of electric connected vehicles (ECVs) traffic stream.

Nevertheless, to get rid of this unreasonable assumption and further promote the integration between CV technology and CF theory, Gong et al. [21] developed a novel platoon CF control scheme based on constrained optimization and distributed computation with the propagation of traffic fluctuation/oscillation being reduced. Ge et al. [22] presented a connected cruise control (CCC) strategy based on a connected CF model to improve the string stability of vehicle platoons with the help of CV technologies. According to the model of the CF behavior for traffic stream, Jia et al. [23] proposed a cooperative driving strategy considering the local traffic information and the downstream traffic information to enhance traffic efficiency and safety. Moreover, Li et al. [12] proposed a novel non-lane-discipline-based CF model considering the effect of lateral gap and roadside device under the V2I-based CV environment.

In the vehicle platoon control field, there are some studies

This work was supported in part by the National Key Research and Development Program under Grants 2018YFB1600500 and 2016YFB0100906 and the National Natural Science Foundation of China under Grants U1964202, 61773082 and Grant 71771200.

H. Zhao and Y. Li are with the Key Laboratory of Intelligent Air-Ground Cooperative Control for Universities in Chongqing, College of Automation, Chongqing University of Posts and Telecommunications, Chongqing 400065, China (e-mail:zhaohang128112@163.com; liyongfu@cqupt.edu.cn).

W. Hao is with the School of Traffic & Transportation Engineering, Changsha University of Science & Technology, Changsha, Hunan 410114, China (e-mail: haowei@csust.edu.cn)

S. Peeta is with the Schools of Civil and Environmental Engineering and Industrial and Systems Engineering, Georgia Institute of Technology, Atlanta, GA 30332 USA (e-mail: peeta@gatech.edu).

Y. Wang is with College of Civil Engineering and Architecture, Zhejiang University, Hangzhou 310058, China (e-mail: wangyibing@zju.edu.cn).

discussing the relationship between dynamic performance of traffic stream and CV technology, which partly motivates this study. Zheng et al. [24] incorporated the communication topology into a platoon control algorithm to enhance internal stability and scalability of homogeneous vehicular platoons. Salvi et al. [25] designed a decentralized consensus protocol for platooning in the presence of time-varying delays and the switching communication topologies. Li et al. [26] proposed a pinning control-based consensus protocol by impropriating the CF interactions between CVs under fixed and the switching communication topologies. Their findings investigate the performance of their strategies on convergence and stability of CV platoon in case of time-variant leader or time-variant leader under fixed or the switching communication topologies.

In addition, the research on EC of EVs has been a hot issue in recent years. For instance, Wu et al. [27] proposed an EC model to extrapolate the power loss of separate electric vehicles in acceleration phase and its power recuperation in deceleration phase. However, the EC for ECVs traffic stream is not linearly related to the EC for an individual EV due to the interactions of CF behavior among vehicles.

The aforementioned studies have preliminarily discussed the integration between CV technology and CF theory. Although there is still a lack of discussion with the relationship between CV environment and communication topology structure. Furthermore, very few of the CF literature are concerned with the CF behavior associated with EC and dynamic performance of traffic stream in an unstable CV environment.

Considering the above issues, this study will make the following contributions:

- A method of combining beacon transmission mechanism, graph theory and probability theory is proposed to characterize the communication connections among ECVs in the context of CV environment.
- A new CF model incorporating the effects of the communication topologies and delays is proposed to describe the behavior of ECVs. In addition, the stability of the proposed CF model is rigorously analyzed by utilizing the perturbation method.
- Extensive simulations are performed to investigate the influence of different communication topologies with switching periods and different delays on dynamic performance and EC of ECVs.

The rest of this paper is structured as follows. Section II introduces a connected environment-based communication topology characterization approach and describes three special cases (i.e., the predecessor following (PF) communication topology, the two-predecessor-leader following (TPLF) communication topology and the switching communication topologies.) to describe the stable/unstable CV environment. Section III develops a CF model incorporating the effects of the communication topologies and delays. Section IV performs the stability analysis of the proposed CF model. Section V presents an EC model includes the power loss and power recuperation. Section VI conducts the numerical experiments with evaluations and the final section summarizes the conclusions together with the future research.

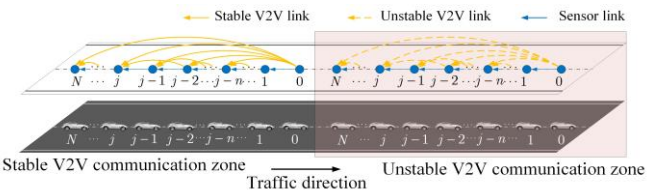

Fig. 1. ECVs move in accordance with CF model from stable V2V communication zone to unstable V2V communication zone

II. General Communication Topology Characterization

This section explains a dedicated short-range communication (DSRC)-based communication topology approach using the adjacent matrix to describe the characteristics of communication topology. Additionally, methods including two typical fixed communication topologies and a switching communication topology are introduced based on the communication topology characterization approach.

A. Beacon Transmission Analysis

As shown in Fig. 1, there is a traffic stream composed of $N+1$ EVs under a CV environment. Vehicle 0 is the leader, and the following vehicles are numbered in ascending order. Vehicle j ($j \in [1, N]$) is the objective following vehicle selected by random method. If j=1 , vehicle j only considers the effect of the leader. In this paper, we study a complex traffic scenario that considers the effects of multiple preceding vehicles. Hence, for convenience, n is defined as $n \in [1, j]$. Vehicle $j-n$ is the *n*th preceding vehicle of vehicle j (see Fig. 1).

Based on our previous study [11], this study makes the following definitions: γ is defined as the slot time, B is the beacon length, R is the data rate, T_h is the duration of the physical layer convergence protocol preamble and header, T_{AIFS} is a time interval between frames being transmitted, T_{EIFS} is the cost time when the physical layer indicates a beacon is unsuccessfully transmitted, T_{CCH} and T_g are the durations of the control channel (CCH) interval and the guard time, respectively. Moreover, $T_S = (T_h + B/R + T_{AIFS})/\gamma$ is the time duration of a successful transmission measured in slot time. $T_c = (T_h + B/R + T_{EIFS})/\gamma$ is the time duration of data collision. $T = (T_{CCH} - T_g - T_h - B/R)/\gamma - T_w$ is a useful duration. And T_w is the backoff time randomly selected from the contention window W , formulating as follows [11, 33]:

$$T_w = \begin{cases} W-1 & for\ N=0 \\ T_s + W - 2 & for\ N=1 \\ NT_s + (W-N-1) & for\ 1<N\le W-1 \\ (N+1-floor(\frac{N+1-W}{2}))T_s & \\ \quad +floor(\frac{N+1-W}{2})T_c & for\ W-1<N<2W \\ (W-1)T_c & for\ N\ge 2W \end{cases}, \tag{1}$$

where $floor(\tilde{x})$ returns the closest integer less or equal than $\tilde{x}$.

Then, the transmission probability $\tilde{p}(l,N+1,W,K)$ ($l\in[1,W]$ and $K\in[2,N+1]$)of a traffic stream is defined, which implies that vehicles in the communication network select back off time in a contention window W, but only K vehicles transmit in the l th slot. The relationship can be formulated as:

$$\begin{aligned}\tilde{p}(l,N+1,W,K) = & [1-\sum_{t=0}^{l-1} p(T_{\tilde{t}}=\tilde{t})]^{N+1}\binom{N+1}{K} \\ \times & [\frac{p(T_{\tilde{t}}=l)}{1-\sum_{t=0}^{l-1} p(T_{\tilde{t}}=\tilde{t})}]^{K} \times [1-\frac{p(T_{\tilde{t}}=l)}{1-\sum_{t=0}^{l-1} p(T_{\tilde{t}}=\tilde{t})}]^{N+1-K}\end{aligned}, \tag{2}$$

where $p(T_{\tilde{t}}=\tilde{t})=1/W$ is defined as the probability of the transmission start time and $\tilde{t}$ is the slots left in this interval. $\sum_{t=0}^{l-1} p(T_{\tilde{t}}=\tilde{t})$ denotes the probability that $(l-1)$ slots pass before the first transmission attempt, and $p(T_{\tilde{t}}=l)/(1-\sum_{t=0}^{l-1} p(T_{\tilde{t}}=\tilde{t}))$ denotes the probability of choosing any slot in the remaining $(T+W-1)$ slots.

Furthermore, the mean number $X(t,N+1)$ of the ECV traffic stream is related to $\tilde{p}(l,N+1,W,K)$, which is:

$$\begin{aligned}X(\tilde{t},N+1) = & \sum_{l=0}^{t}(\tilde{p}(l,N+1,W,1)(1+X(\tilde{t}-l+1-T_s,N+1))) \\ & +\sum_{K=2}^{N+1}(\tilde{p}(l,N+1,W,K)X(\tilde{t}-l+1-T_s,N+1-K))\end{aligned}, \tag{3}$$

Therefore, a probability of a successful beacon delivery of vehicle j is calculated by:

$$p_j = \frac{X(\tilde{t},N)}{N}, \tag{4}$$

where $X(t,N)$ is the mean number of N ECVs(except vehicle j) that successfully transmit beacons during each CCH interval.

B. General Communication Topology

To make up for the aforementioned deficiencies, the DSRC-based V2V communication signal strength between vehicle j and vehicle $j-n$ is defined as follows:

$$q_{j,j-n} = \begin{cases} \sigma(1-\frac{\Delta x_{j,j-n}}{L}) & for\ \ \Delta x_{j,j-n}<L \\ 0 & for\ \ \Delta x_{j,j-n}\ge L \end{cases} \tag{5}$$

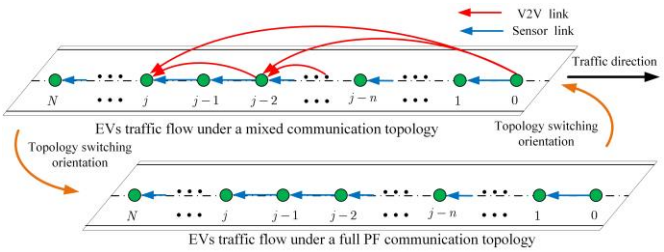

Fig. 2. The mixed communication topology cyclical switching process in unstable V2V communication zone

where $\Delta x_{j,j-n}$ represents the space headway between vehicle j and vehicle $j-n$, L is the maximum communication range of onboard unit (OBU). $\sigma\in[0,1]$ is defined as the interference coefficient related to communication environment. If the communication environment is favorable, then σ=1 . Additionally, $0\le\sigma<1$ denotes that the communication signal suffers from external interference, such as buildings, thunderstorms, etc. σ=0 denotes communication signal has been cut off due to intense interference.

If $q_{j,j-n}>0$, the communication connections are asserted to possess a chance to be established. Further, $\xi_{j,j-n}=1$ represents the connection between vehicle j and vehicle $j-n$ has been established. And $\xi_{i,i-n}=0$ otherwise.

Based on Eqs. (4) and (5), the probability function for the V2V communication connection can be derived as follows:

$$Q_{j,j-n}(\xi_{j,j-n}=1\,|\,q_{j,j-n}>0) = p_j \times f(q_{j,j-n},\Delta x_{j,j-n},L,\cdots), \tag{6}$$

where $Q_{j,j-n}$ is the probability that vehicle j can obtain the information from vehicle $j-n$. Considering non-ignorable interference and packet loss, the connection is reliable when the probability reaches a certain standard. To be specific, we define the Heaviside step function as follows:

$$\theta_{j,j-n} = \Theta(Q_{j,j-n}-\mu), \tag{7}$$

where μ is the threshold value to distinguish the probability values of reliable communication connections and those of unreliable communication connections. Particularly, this study uses μ=0.6 to ensure that reliable information exchange can occur between vehicles [11, 33]. Additionally, $\theta_{j,j-n}$ (which is equal to 0 for $Q_{j,j-n}<\mu$ and equal to 1 otherwise) serves as the parameter for information exchange. $\theta_{j,j-n}=1$ represents vehicle j can obtain the information from vehicle $j-n$, and this connection is reliable. And $\theta_{j,j-n}=0$ otherwise.

Consequently, the communication topology can be described by an adjacent matrix as follows:

$$A = \begin{bmatrix} \theta_{0,0} & \cdots & \cdots & \theta_{0,N} \\ \vdots & \ddots & \vdots & \vdots \\ \vdots & \vdots & \ddots & \vdots \\ \theta_{N,0} & \cdots & \cdots & \theta_{N,N} \end{bmatrix}. \tag{8}$$

Noted that, $\theta_{j,j-1}=1$ represents that vehicle j can sense the information of the nearest preceding vehicle $j-1$ via sensors. According to [28, 29], the sensors for real-time traffic are reliable, that is, the value of $\theta_{j,j-1}$ is 1. In addition, the value of $\theta_{j,j}$, which denotes that vehicle j obtains information from itself, is considered as 1 in this paper.

C. The Fixed Communication Topology Description

Considering the scenario of an ECV traffic stream under a CV environment shown in Fig. 1, the lower layer shows the vehicle movement in the physical space while the upper layer indicates the communication topology in cyber space. If V2V communication is stable, the connection link in cyber space is in accordance with the TPLF communication topology, which means that each vehicle has access to information of its immediate predecessor via the unidirectional sensor link, and its next immediate predecessor via the V2V link, as well as the leader via the V2V link. According to Eq. (4), it can be characterized as follows:

$$A_{TPLF}=\begin{bmatrix} \theta_{0,0} & \theta_{0,1} & \theta_{0,2} & \cdots & \cdots & \cdots & \theta_{0,N} \\ 0 & \theta_{1,1} & \theta_{1,2} & \theta_{1,3} & 0 & \cdots & 0 \\ \vdots & \vdots & \ddots & \ddots & \ddots & \cdots & \vdots \\ \vdots & \vdots & \cdots & \ddots & \ddots & \ddots & 0 \\ \vdots & \vdots & \cdots & \cdots & \ddots & \ddots & \theta_{N-2,N} \\ 0 & \vdots & \cdots & \cdots & \cdots & \theta_{N-1,N-1} & \theta_{N-1,N} \\ 0 & 0 & \cdots & \cdots & \cdots & 0 & \theta_{N,N} \end{bmatrix}. \quad (9)$$

The PF communication topology denotes each vehicle in the traffic stream will only access to the information via the unidirectional sensor link. That is:

$$A_{PF}=\begin{bmatrix} \theta_{0,0} & \theta_{0,1} & 0 & \cdots & \cdots & \cdots & 0 \\ 0 & \theta_{1,1} & \theta_{1,2} & 0 & 0 & \cdots & 0 \\ \vdots & \vdots & \ddots & \ddots & \ddots & \cdots & \vdots \\ \vdots & \vdots & \cdots & \ddots & \ddots & \ddots & 0 \\ \vdots & \vdots & \cdots & \cdots & \ddots & \ddots & 0 \\ 0 & \vdots & \cdots & \cdots & \cdots & \theta_{N-1,N-1} & \theta_{N-1,N} \\ 0 & 0 & \cdots & \cdots & \cdots & 0 & \theta_{N,N} \end{bmatrix}. \quad (10)$$

D. The Switching Communication Topology

As shown in Fig.2, supposing that the ECV traffic stream is under a mixed communication topologies consisting of PF and TPLF topologies. Besides, a sinusoidal interference is considered, which will lead to periodic switching of the communication topologies. In this study, we consider the scenario of ECVs that can perceive information via DSRC communications and sensors, and its communication topology switches from the TPLF communication topology→ the PF communication topology→the TPLF communication topology⋯. Accordingly, the corresponding adjacent matrix A of each TPLF communication topology is also changed according to the switching direction.

III. Car-following Model Derivation

Based on the scenario under investigation shown in Fig. 1, each vehicle can have access to the information related to position and velocity from surrounding vehicles via V2V-based or sensor-based connection link. Based on the communication topology characterization discussed in Section II, a new CF model incorporating the different communication topologies and heterogeneous delays is formulated as follows [12, 15]:

$$\begin{aligned} a_j(t)=k(&\sum_{n=1}^{j}C_{j,j-n}\alpha_{j,j-n} \\ &\times V_{j,j-n}(\Delta x_{j,j-n}(t-\tau_{j,j-n}))-v_j(t-\varsigma_j)), \\ &+\lambda(\sum_{n=1}^{j}C_{j,j-n}\alpha_{j,j-n}\Delta v_{j,j-n}(t-\varsigma_{j,j-n})) \end{aligned} \quad (11)$$

where $x_j(t)$, $v_j(t)$, $a_j(t)$ represent the position (m), velocity ($\mathrm{m/s}$) and acceleration ($\mathrm{m/s^2}$) of the vehicle j at time t, respectively. $t\in\mathbb{R}$ represents the time (s). $\Delta x_{j,j-n}(t)\equiv x_{j-n}(t)-x_j(t)$, $\Delta v_{j,j-n}(t)\equiv v_{j-n}(t)-v_j(t)$ are the longitudinal position difference and the velocity difference between the preceding vehicle $j-n$ and the follower vehicle j at time t, respectively. $\tau_{j,j-n}$, ς_j and $\varsigma_{j,j-n}$ are delays with respect to $\Delta x_{j,j-n}$, v_j, and $\Delta v_{j,j-n}$ respectively. $k\geq 0$ and $\lambda\geq 0$ are sensitivity coefficients.

$C_{j,j-n}$ denotes communication connection parameter between the preceding vehicle $j-n$ and vehicle j. According to Eq. (8), it can be determined as:

$$C_{j,j-n}=\begin{cases} 1 & \theta_{j,j-n}=1 \ and \ \theta_{j-n,j}=1 \\ 1 & \theta_{j,j-n}=1 \ and \ \theta_{j-n,j}=0 \\ 0 & \theta_{j,j-n}=0 \ and \ \theta_{j-n,j}=1 \\ 0 & \theta_{j,j-n}=0 \ and \ \theta_{j-n,j}=0 \end{cases}. \quad (12)$$

In addition, α is the weight value, which is used to distinguish the deviations' effect of different preceding vehicles on CF behavior. Unlike the definitions in [12, 14, 17], which are just concerned with the space position of predecessors, the additional V2V communication connection parameter $C_{j,j-n}$ is also considered in this study for matching the changes of the weight values with the connection/disconnection among vehicles. That is:

$$\alpha_{j,j-n}=\begin{cases} \dfrac{C_{j,0}}{(j+1)^{j-1}} & for \ n=j \\ \dfrac{jC_{j,n}}{(j+1)^{n}} & for \ n\in[2,j-1] \\ 1-\dfrac{C_{j,0}}{(j+1)^{j-1}}-\sum_{\psi=2}^{j-1}\dfrac{jC_{j,j-\psi}}{(j+1)^{\psi}} & for \ n=1 \end{cases}. \quad (13)$$

The values of $\alpha_{j,j-n}$ are in accordance with the changes of influence from the immediately preceding vehicle to the leader. In other words, the further of the distance between the objective

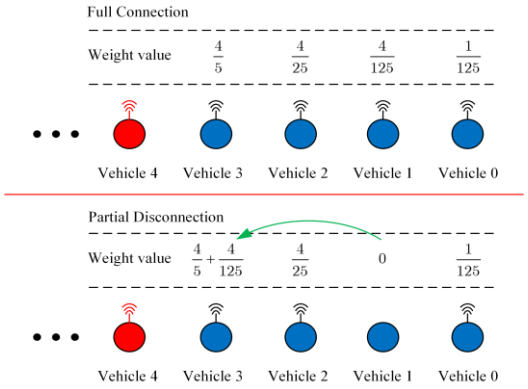

Fig. 3. Illustration of weight allocation.

vehicle and the preceding vehicle is, the weaker of the influence is. To further facilitate the understanding Eq. (13), Fig. 3 vehicle 4 in a traffic stream as an example. For safety, when the connection state among vehicles changes from the full connection to the partial disconnection, according to Eq. (13), it will suggest taking the weight of the disconnected vehicle (e.g. vehicle 1 in Fig. 3) away and assigning it to the immediately preceding vehicle.

In addition, the optimal velocity function is [12, 15, 26, 30]:

$$V(\Delta x) = V_1 + V_2(\tanh(S_1(\Delta x - l_c) - S_2)), \quad (14)$$

where V_1, V_2, S_1 and S_2 are constant parameters, l_c is the vehicle length, and $\tanh(\xi)=\dfrac{e^{\xi}-e^{\xi}}{e^{\xi}+e^{\xi}}$ is the hyperbolic tangent function (ξ is a rational number), and Δx in $V(\Delta x)$ is a function to be determined.

Remark 1. Based on the proposed model in Eq. (11), if the connection link is in accordance with the TPLF communication topology, and this model will be rewritten as follows:

$$\begin{aligned} a_j(t) = k(&\alpha_{j,j-1}V_{j,j-1}(\Delta x_{j,j-1}(t-\tau_{j,j-1})) \\ &+\alpha_{j,j-2}V_{j,j-2}(\Delta x_{j,j-2}(t-\tau_{j,j-2})) \\ &+\alpha_{j,0}(V_{j,0}(\Delta x_{j,0}(t-\tau_{j,0})) - v_j(t-\varsigma_j)) \\ &+\lambda(\alpha_{j,j-1}\Delta v_{j,j-1}(t-\varsigma_{j,j-1}) \\ &+\alpha_{j,j-2}\Delta v_{j,j-2}(t-\varsigma_{j,j-2}) + \alpha_{j,0}\Delta v_{j,0}(t-\varsigma_{j,j-2})) \end{aligned} \quad .(15)$$

If the communication connections switch to the PF communication topology, and this model will be reduced to:

$$\begin{aligned} a_j(t) = k(&V_{j,j-1}(\Delta x_{j,j-1}(t-\tau_{j,j-1})) - v_j(t-\varsigma_j)) \\ &+\lambda\Delta v_{j,j-1}(t-\varsigma_{j,j-1}) \end{aligned} \quad . (16)$$

If delays of the CF model in Eq. (16) are assumed to be zero(i.e. $\tau_{j,j-1}=\varsigma_j=0$ s), the model will be similar to the existing CF model in [15]. These findings prove that the full velocity difference (FVD) model is a special case of the proposed model.

IV. Stability Analysis

In this section, the perturbation method [12, 31] is used to analyze the stability of the proposed CF model with the purpose to obtain the stability condition.

Assumption. The initial state of the traffic stream is a uniform equilibrium stream. All ECVs in the traffic stream travel with the identical space headway h and the optimal velocity $V(h)$.

Theorem. The general stability condition of uniform traffic stream in Eq. (11) is:

$$V'(h) < \frac{G}{W}, \quad (17)$$

$$G = k\sum_{n=1}^{j} C_{j,j-n}\alpha_{j,j-n}n^2 + 2\lambda(\sum_{n=1}^{j} C_{j,j-n}\alpha_{j,j-n}n)^2, \quad (18)$$

$$\begin{aligned} W = 2(&\sum_{n=1}^{j} C_{j,j-n}\alpha_{j,j-n}n)(k\sum_{n=1}^{j} C_{j,j-n}\alpha_{j,j-n}n\tau_{j,j-n} \\ &+\sum_{n=1}^{j} C_{j,j-n}\alpha_{j,j-n}n(1-k\varsigma_j)) \end{aligned} \quad . \quad (19)$$

And the stability condition of the uniform ECVs traffic stream under the TPLF communication topology in Eq. (15) is:

$$V'(h)_{TPLF} < \frac{G_{TPLF}}{W_{TPLF}}, \quad (20)$$

$$\begin{aligned} G_{TPLF} = &k(\alpha_{j,j-1} + 4\alpha_{j,j-2} + j^2\alpha_{j,0}) \\ &+2\lambda(\alpha_{j,j-1} + 2\alpha_{j,j-2} + j\alpha_{j,0})^2 \end{aligned}, \quad (21)$$

$$\begin{aligned} W_{TPLF} = &2(\alpha_{j,j-1} + 2\alpha_{j,j-2} + j\alpha_{j,0}) \\ &\times(k(\alpha_{j,j-1}\tau_{j,j-1} + 2\alpha_{j,j-2}\tau_{j,j-2} + j\alpha_{j,0}\tau_{j,0}) \\ &+(1-k\varsigma_j)(\alpha_{j,j-1} + 2\alpha_{j,j-2} + j\alpha_{j,0})) \end{aligned} \quad . \quad (22)$$

If the TPLF communication topology is switched to the PF communication topology. The stability condition of the uniform ECVs traffic stream in Eq. (16) is:

$$V'(h)_{PF} < \frac{k+2\lambda}{2k(\tau_{j,j-1}-\varsigma_j)+2}. \quad (23)$$

Proof. Based on the assumption, the position solution to the steady traffic stream is:

$$x_j^0(t) = h(N-j) + V(h)t, \quad (24)$$

where h is the steady headway, and $x_j^0(t)$ is the position of the j th vehicle at steady state.

Adding a small disturbance $y_j(t)$ to $x_j^0(t)$, i.e.,

$$x_j(t) = y_j(t) + x_j^0(t). \quad (25)$$

Substituting Eq. (25) into Eq. (11) and linearizing the resulting equation using the Taylor expansion, it follows that:

$$\begin{aligned} \ddot{y}_j(t) = k(&V'(h)\sum_{n=1}^{j} C_{j,j-n}\alpha_{j,j-n} \times \Delta y_{j,j-n}(t-\tau_{j,j-n}) - \dot{y}_j(t-\varsigma_j)) \\ &+\lambda(\sum_{n=1}^{j} C_{j,j-n}\alpha_{j,j-n}\Delta\dot{y}_{j,j-n}(t-\varsigma_{j,j-n})) \end{aligned} \quad . \quad (26)$$

Set $y_j(t)$ in the Fourier models, i.e., $y_j(t) = Ae^{\mathrm{i}\beta(N-j)+zt}$, where β is the wavenumber ($0 \le \beta \le \pi$), $z = \mathrm{i}\omega$, and ω is the wave angular frequency. Substituting it in Eq. (26), the resulting equation is:

$$\begin{aligned} z^2 &= k(\sum_{n=1}^{j} C_{j,j-n}\alpha_{j,j-n}V'(h)(1-z\tau_{j,j-n}) \\ &\times(ni\beta+\frac{n^2}{2}(i\beta)^2)-z(1-z\varsigma_j)) \\ &+\lambda(\sum_{n=1}^{j} C_{j,j-n}\alpha_{j,j-n}z(1-z\varsigma_{j,j-n})(ni\beta+\frac{n^2}{2}(i\beta)^2)) \end{aligned} \quad , \quad (27)$$

Let $z = z_1(i\beta) + z_2(i\beta)^2 + \cdots$, and substitute it into Eq. (27), it has:

$$\begin{aligned} &z_1^{\,2}(i\beta)^2 + 2z_1z_2(i\beta)^3 + z_2^{\,2}(i\beta)^4 = k(\sum_{n=1}^{j} C_{j,j-n}\alpha_{j,j-n}V'(h) \\ &\times(1-(z_1(i\beta)+z_2(i\beta)^2)\tau_{j,j-n})(i\beta n+\frac{n^2}{2}(i\beta)^2) \\ &-(1-(z_1(i\beta)+z_2(i\beta)^2)\varsigma_j)(z_1(i\beta)+z_2(i\beta)^2)) \\ &+\lambda(z_1(i\beta)+z_2(i\beta)^2)(\sum_{n=1}^{j} C_{j,j-n}\alpha_{j,j-n} \\ &\times(1-(z_1(i\beta)+z_2(i\beta)^2)\varsigma_{j,j-n})(i\beta n+\frac{n^2}{2}(i\beta)^2)) \end{aligned} \quad . \quad (28)$$

Combining similar items in terms of $(i\beta)$, for simplicity, hereafter, we denote $z_1(i\beta)$ and $z_2(i\beta)$ as z_1 and z_2, respectively. It follows from Eq. (28) that

$$\begin{cases} z_1 = V'(h)\sum_{n=1}^{j} C_{j,j-n}\alpha_{j,j-n}n \\ z_2 = \sum_{n=1}^{j} C_{j,j-n}\alpha_{j,j-n}V'(h)(\frac{n^2}{2}-nz_1\tau_{j,j-n})+z_1^{\,2}\varsigma_j \\ \quad +\frac{\lambda}{k}(z_1\sum_{n=1}^{j} C_{j,j-n}\alpha_{j,j-n}n)-\frac{1}{k}z_1^2 \end{cases} . \quad (29)$$

According to the long-wavelength method, when $z_1 > 0$ and $z_2 > 0$, the neutral stability condition in Eqs. (17)-(19) is derived.

Remark 2. Based on Inequation (17), if the V2V link is in accordance with the TPLF communication topology, which means just $C_{j,j-1}$=1, $C_{j,j-2}$=1 and $C_{j,0}$=1. Hence, the neutral stability condition is given by Eqs. (20)-(22). If the V2V link is in accordance with the PF communication topology, which means just $C_{j,j-1}$=1. Hence, the neutral stability condition is given by Inequation. (23).

V. Energy Consumption Model

The energy system of an electric vehicle can be simplified to two subsystems. One of which is power loss consumed by the travel resistance, motor, and ancillaries. Another one is power recuperation, as an ECV can recuperate a part of the kinetic energy lost during the deceleration phase to recharge the battery. Hence, this section introduces an evaluation approach with respect to the EC of ECVs traffic stream. The EC model considers both power loss and power recuperation.

A. Power Loss P_l

Travel resistance: The required tractive effort can be described as follows [12, 13, 27]:

$$F = Ma + \delta v^2 + f_r Mg + \frac{bv}{R_t}, \quad (30)$$

where F is the tractive effort (in N); M is the vehicle mass (in kg); a is the vehicle acceleration (in $\mathrm{m/s^2}$); v is the vehicle velocity (in $\mathrm{m/s}$); $\delta = 0.5\rho C_D A_f$ is an aerodynamic resistance constant determined by air density ρ (in $\mathrm{kg/m^3}$), frontal area of the vehicle A_f (in $\mathrm{m^2}$) and coefficient of drag C_D. f_r is rolling resistance constant and g is gravity acceleration ($g = 9.81\ \mathrm{m/s^2}$); b is the bearings' damping coefficient (in m) and R_t is the effective electric vehicle tire radius (in m).

Motor: The traffic effort F generated by the torque of the motor can be simplified as a product of the armature constant, magnetic flux, current, which can be formulated as [12, 13, 27]:

$$F = \frac{K \bullet I}{R_t}, \quad (31)$$

where $K = K_a\phi_d$; K_a is the armature constant; ϕ_d is the magnetic flux (in webe); I is the current (in A).

Ancillaries: Some other electric devices equipped in vehicles may use a part of the electric energy. Thus, the ancillary power loss P_a is given by [12, 13, 27]:

$$P_a = P_{ac} + P_{bm} + P_{el} + P_{au}, \quad (32)$$

where P_{ac}, P_{bm}, P_{el}, P_{au} are ECs of air-conditioner, battery management, external lights and audio, respectively. Note that all of the above ancillary ECs are independent of velocity.

Consequently, the electric vehicle power loss can be obtained as follows [12, 13, 27]:

$$\begin{aligned} P_l = &\frac{r \cdot R_t^{\,2}}{K^2}(Ma + \delta v^2 + f_r Mg + \frac{bv}{R_t})^2 \\ &+(\delta v^2 + f_r Mg + \frac{bv}{R_t})v + P_a \end{aligned} \quad , \quad (33)$$

where the r is the resistance of the conductor (in Ω).

B. Power Recuperation P_r

Electric vehicles can recharge their batteries by applying negative torque to their drive wheels and converting kinetic energy to electrical energy. However, the process of converting from kinetic energy to electrical energy is not equivalent. Hence, taking η to represent the efficiency of the generator and the regenerative braking power is [12, 13, 27]:

$$P_r = \eta \cdot Mav. \quad (34)$$

Hence, the EV's instantaneous power is [12, 13, 27]:

$$P = P_l + P_r. \quad (35)$$

VI. Numerical Experiments

The Matlab 9.0-based numerical experiments adopt the CF model and EC model in this study to demonstrate the effects of

different communication topology switching periods and delays on the dynamic performance and EC of the ECVs traffic stream in a CV environment, respectively. To this end, we consider a scenario of mixed communication topologies consisting of PF and TPLF topologies in a fifteen electric connected vehicles (ECVs) platoon. In particular, vehicle 0, 3, 7, and 11 are specified ECVs, and the TPLF commutation topology is utilized to characterize the connections among them with the aid of DSRC communications and sensors. Accordingly, the PF topology is utilized to characterize the connections among the rest vehicles with the aid of sensors. (see Fig. 2).

Meanwhile, the initial states of all vehicles are set as 18.3 m (space headway between two adjacent vehicles), 8 m/s (velocity), 0 m/s^2 (acceleration). Then, the leader begins to operate by [30]:

$$v_0(t)=\begin{cases}8+\dfrac{6.6}{1+e^{-0.35t+38}}\,\mathrm{m/s}, & 0\mathrm{s}\le t<150\mathrm{s}\\ 14.6-\dfrac{6.6}{1+e^{-0.35t+63}}\,\mathrm{m/s}, & 150\mathrm{s}\le t<300\mathrm{s}\end{cases}. \quad (36)$$

Additionally, all the following ECVs start to run according to proposed CF model in Eq. (11).

To perform the following simulations, the values of relevant parameters in Eqs. (11) and (35) are given in Table I and Table II [11, 12, 19, 22, 27, 33].

A. The Effects of Switching Period

In order to evaluate the effects of switching period on communication connection state, dynamic performance and EC, three types of interferences are considered to investigate the impacts the V2V connections among vehicles 0, 3, 7, and 11. In particular, those interferences are characterized as no interference, slight periodic interference (a sinusoidal interference with 20π s-period) and strong periodic interference (a sinusoidal interference with 4π s-period). Besides, the peak and valley of the periodic interferences in the following Figs. 6 and 8 are respectively corresponding to $\sigma=0$ and $\sigma=1$ in Eq. (5). Meanwhile, the connection values in Figs. 6 and 8 denote the connected communication (i.e., 1) and disconnected communication (i.e., 0).

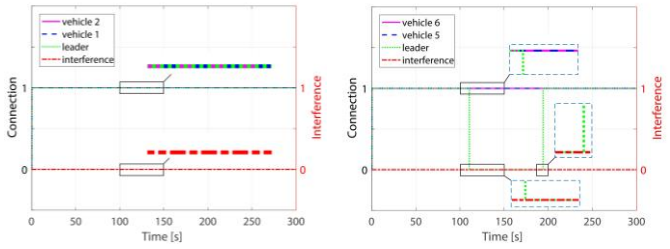

(a) (b)

TABLE I
IEEE 802.11P PARAMETERS [11, 33]

Parameter	Value	Unit	Parameter	Value	Unit
Channel width	10	MHz	Symbol duration	8	μs
Guard time	1.6	μs	EIFS	188	μs
Slot time	16	μs	AIFS	71	μs
Contention Window	8	--	Beacon frequency	10	Hz
Header duration	40	μs	CCHI	46	ms
Beacon size	64	bytes	Chanel data rate	6	Mbps
Reliable threshold value	0.6	--	Maximum communication distance	1000	m

TABLE II
VALUES OF THE RELEVANT PARAMETERS IN CF MODEL AND EC MODEL [12, 15, 16, 27]

Parameter	Value	Unit	Parameter	Value	Unit
M	1500	kg	b	1.0	m
f_r	0.015	--	P_a	2.0	kw
C_D	0.3	--	k	1.5	s^{-1}
A_f	1.8	m^2	λ	0.9	s^{-1}
ρ	1.2	kg/m^3	V_1	6.75	m/s
r	0.11	Ω	V_2	7.91	m/s
η	0.3	--	S_1	0.13	m^{-1}
g	9.81	m/s^2	S_2	1.57	--
R_t	0.3	m	l_c	5.0	m

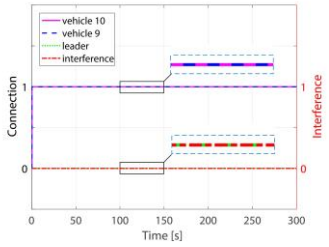

(c)

Fig. 4. The connection state without interference: (a) vehicle 3; (b) vehicle 7; (c) vehicle 11

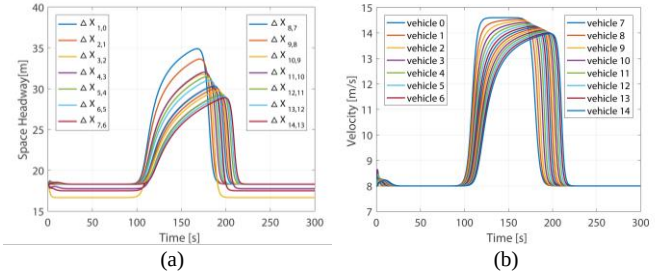

(a) (b)

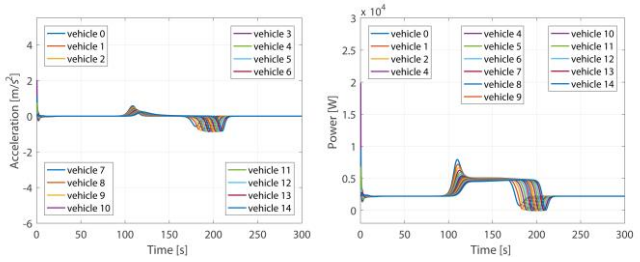

(c) (d)

Fig. 5. The motion state profiles of EV stream without interference: (a) space headway; (b) velocity; (c) acceleration; (d) power consumption

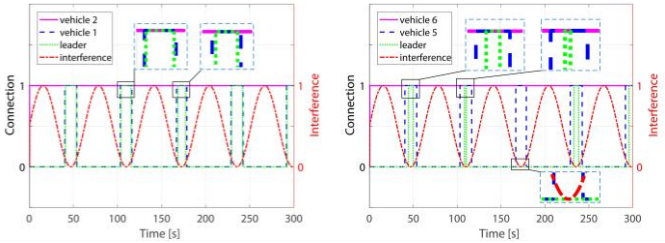

(a) (b)

(c)

Fig. 6. The connection state with slight periodic interference: (a) vehicle 3; (b) vehicle 7; (c) vehicle 11

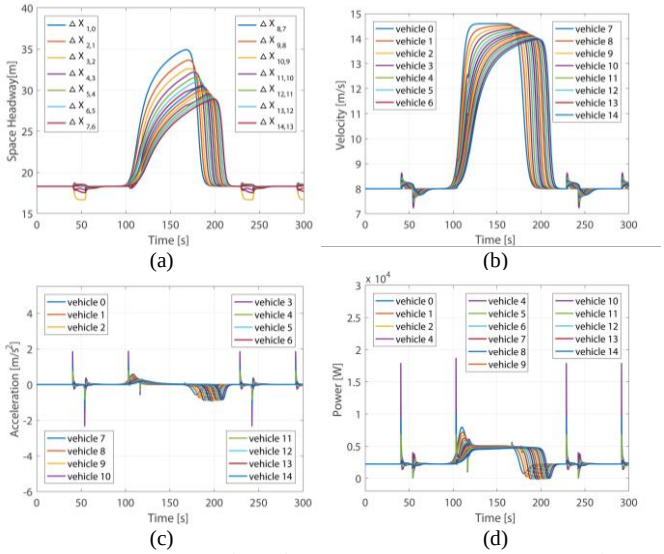

(a) (b)

(c) (d)

Fig. 7. The motion state profiles of EV stream with slight periodic interference: (a) space headway; (b) velocity; (c) acceleration; (d) power consumption

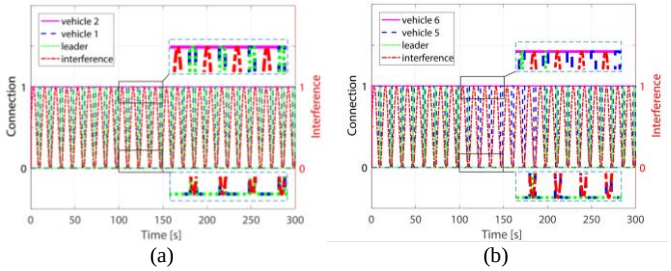

(a) (b)

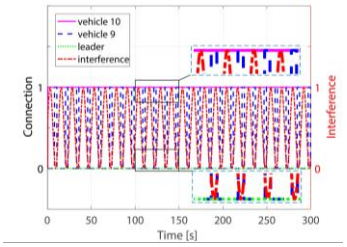

(c)

Fig. 8. The connection state with strong periodic interference: (a) vehicle 3; (b) vehicle 7; (c) vehicle 11

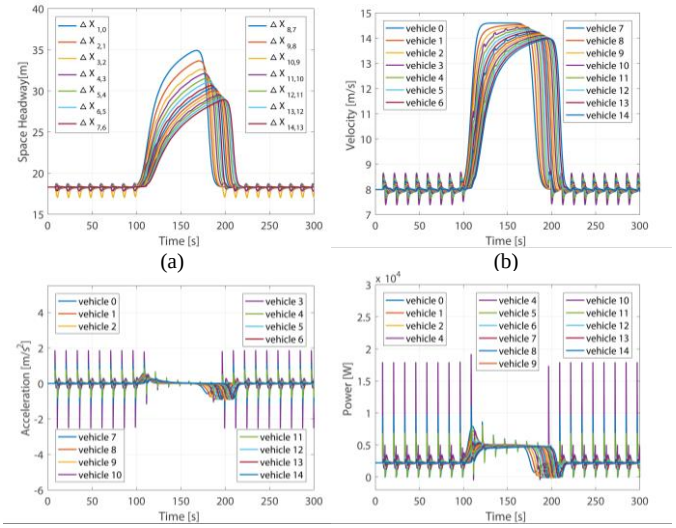

(a) (b)

(c) (d)

Fig. 9. The motion state profiles of EV stream with strong periodic interference: (a) space headway; (b) velocity; (c) acceleration; (d) power consumption

By comparing these above figures, the main findings are summarized as follows:

(i) Connections: The characterization method on communication connection can accurately reproduce the change process of connection states with the changes in vehicle motion states. For instance, Fig. 7(a) and 7(b) shows that the space headway between two vehicles increases with increasing velocity between 100s and 200s. Then, comparing the connection state between vehicle 3 and the leader (the green lines in megascopic subplots of Fig. 6(a)), it implies that the emerging duration of reliable communication connection will contract when the communication distance between two vehicles increases. In addition, the more prominent comparison can be found in Fig. 6(b). Besides, the connection between vehicle 7 and the leader is cut off when the space headway reaches the peaks (at approximately 170 s). While the connection between vehicle 11 and the leader is always in disconnected state due to the large distance in Fig. 6(c). Furthermore, it is logical that the V2V connection between two vehicles in a close range, such as vehicle 3 and vehicle 1, will emerge crosscurrent to the periodic signal interference.

(ii) Dynamic performance: According to the above experiments, a stable communication connection can benefit the smoothness of the traffic stream. In particular, smoothness reflects the number of oscillations in the space headway, velocity or acceleration profile. It is obvious that data in Fig. (5) is much better than that in Fig. (7) and Fig. (9). Besides, the better smoothness signifies a more comfortable driving

TABLE III
EC DATA OF ECVS FOR DIFFERENT PERIODIC SIGNAL INTERFERENCES.

Delay (s)	Interference Period (s)	Total EC (J)
0	∞	13065044.3
	20π	13104819.2
	4π	13223491.9

experience.

(iii) EC: An unstable communication connection causes more EC in an ECV stream. In particular, combining Figs. 4, 6, 8 and Figs. 5, 7, 9, every communication connection/disconnection will result in some surges in velocity and acceleration profiles. Then, it further leads to more energy consumption. Moreover, Table III directly demonstrates that the total energy of the ECVs traffic stream without interference is 13065044.3 J, followed by 13104819.2 J for slight interference with a 20π s-period, and then 13223491.9 J for strong interference with a 4π s-period. These findings further illustrate the significance of stable communication connections in ECVs related to energy saving.

B. *The Effects of Communication Delays*

This section aims to evaluate the effects of communication delays on the dynamic performance and EC of the ECV stream. In CV environment, safety messages, like anti-collision information, need demanding delay requirements. According to [32], the communication delays are set as 0s, 0.1 s and 0.2 s, In addition, the period of interference in this part is set as 20π s. In order to facilitate the explanation, the peaks or valleys of oscillation in the following Figs. 10-12 are calibrated.

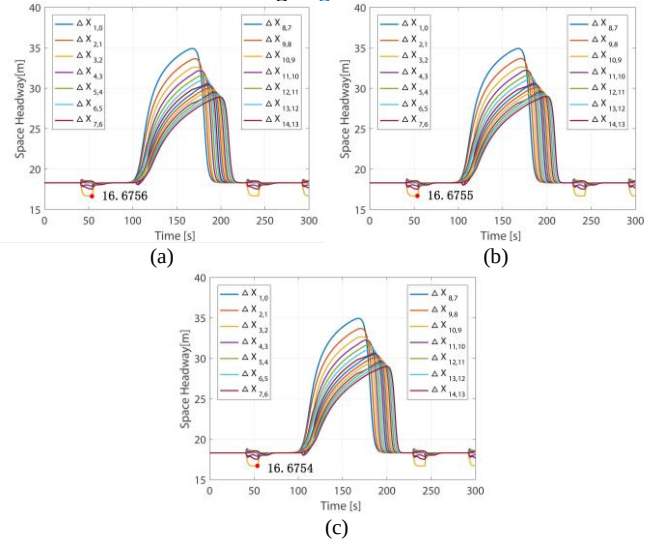

(a) (b) (c)

Fig. 10. The space headway profiles of ECV stream with slight periodic interference and: (a) no delay; (b) delay 0.1 s; (c) delay 0.2 s

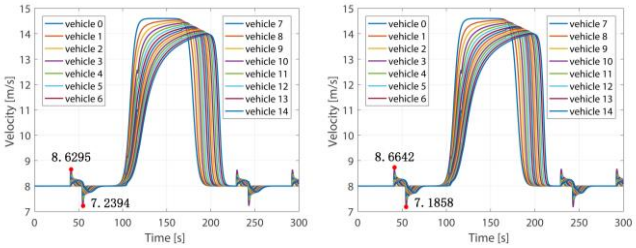

(a) (b)

TABLE IV
EC DATA OF EVS FOR DIFFERENT COMMUNICATION DELAYS

Delay (s)	Interference PERIOD (S)	Total EC (J)
0	20π	13104819.2
0.1		13110785.9
0.2		13117138.6

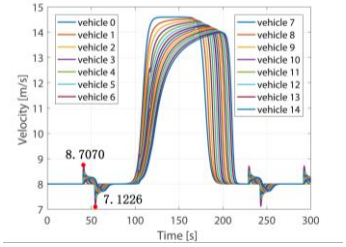

(c)

Fig. 11. The velocity profiles of ECV stream with slight periodic interference and: (a) no delay; (b) delay 0.1 s;(c) delay 0.2 s

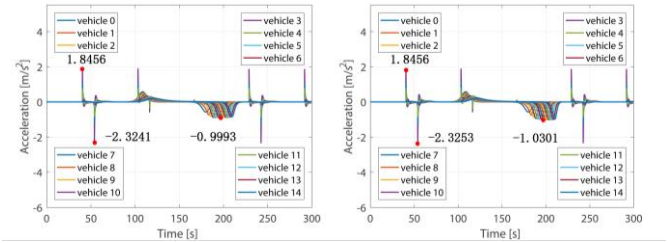

(a) (b)

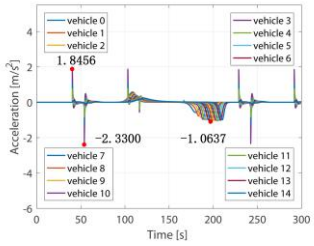

(c)

Fig. 12. The acceleration profiles of ECV stream with slight periodic interference and: (a) no delay; (b) delay 0.1 s; (c) delay 0.2 s

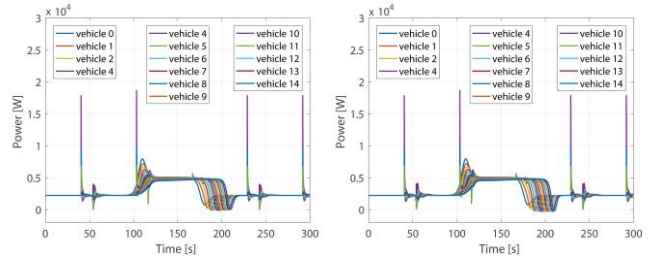

(a) (b)

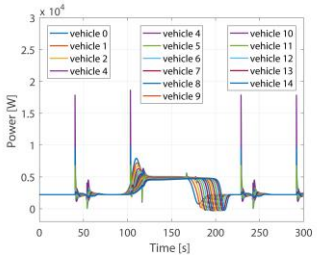

(c)

Fig. 13. The power consumption profiles of ECV stream with slight periodic interference and: (a) no delay; (b) delay 0.1 s; (c) delay 0.2 s

By comparing these above figures, the main findings are

summarized as follows:

(i) Dynamic performance: Based on the proposed CF model, the communication delays negatively impact the smoothness of ECV stream. In particular, although only followers 3, 7, and 11 are suffered from the influences of communication delays, the maximum amplitudes of oscillations in Figs. 10(c)-12(c) are a little larger than those in Figs. 10(a)-12(a) or Figs. 10(b)-12(b). As for an ECV stream, it seems that communication delays will not have such a great impact (like the situation under unstable communication connection environment) on dynamic performance if the minimum delay requirements can be guaranteed.

(ii) EC: Based on the EC characteristics described by the proposed model in Eq. (35), the EC of traffic stream shows a trend to increase with the increasing communication delay. In particular, Table IV illustrates the total EC of the traffic stream without delay is 13104819.2 J, which is smaller than 13110785.9 J with delay 0.1 s, followed by 13117138.6 J with delay 0.2 s. Based on the analytical results of dynamic performance, it can be concluded that the little larger amplitudes in velocity and acceleration profiles are the main reason of the increased EC.

I. Conclusions

In this study, a general CF model incorporating the effects of communication topologies and communication delays has been proposed in a CV environment. According to the theoretical analysis, the stability condition of the proposed CF model is derived. Extensive simulations are performed to illustrate the effects of different switching periods with communication topologies (caused by different interference periods). Moreover, different communication delays are also investigated in terms of the velocity, acceleration and power consumption profiles according to the proposed CF model.

The results verify the effectiveness of the proposed CF model on describing the characteristics of ECVs traffic stream with different communication topologies and delays. In addition, this paper highlights the significance of reliable communication connection on the dynamic performance and EC of ECVs traffic stream. In particular, the dynamic performance (i.e. smoothness) of the proposed model will be deteriorated, and the more energy will be consumed by ECVs with the decreases in switching period. Furthermore, the proposed CF model can also evaluate the influence of the communication delays on dynamic performance and EC.

The findings of this study will provide insights for investigation of the EC of mixed traffic both for ECVs and electric automated vehicles (EAVs) under complex traffic situations. In addition, this study also generates the idea to seek an optimal communication topology for general mixed traffic so that energy can be saved more efficiently.

References

[1] L. Thibault., G. D. Nunzio, A. Sciarretta and V. Li, “A unified approach for electric vehicles range maximization via eco-routing, eco-driving, and energy consumption prediction,” *IEEE Trans. Intell. Transp. Syst.*, vol. 3, no. 4, pp. 463-475, Dec. 2019.

[2] M. Ceraolo, A. d. Donato and G. Franceschi, “A general approach to energy optimization of hybrid electric vehicles,” *IEEE Trans. Veh. Technol.*, vol. 57, no. 3, pp. 1433-1441, May. 2008.

[3] F. Browand, J. McArthur, C. Radovich, "Fuel saving achieved in the field test of two tandem trucks", *California Partners Adv. Transit Highways (PATH)*, pp. UCB-ITS-PRR-2004-20, 2004.

[4] S. Zhang, Y. Luo, K. Li and V. Li, “Real-time energy-efficient control for fully electric vehicles based on an explicit model predictive control method,” *IEEE Trans. Veh. Technol*., vol. 67, no. 6, pp. 4693-4701, Jun. 2018.

[5] C. Zheng, D. Feng, S. Zhang, X. Xia, G. Qian and G. Y. Li, “Energy efficient v2x-enabled communications in cellular networks,” *IEEE Trans. Veh. Technol.*, vol. 68, no.1, pp. 554-564, Jan. 2019.

[6] K. Liang, J. Martensson, K. H. Johansson, "Heavy-duty vehicle platoon formation for fuel efficiency", *IEEE Trans. Intell. Transp. Syst.*, vol. 17, no. 4, pp. 1051-1061, Apr. 2016.

[7] S. Tsugawa, S. Jeschke, S. E. S, “A review of truck platooning projects for energy savings,” *IEEE Trans. Intell. Transp. Syst*., vol. 1, no. 1, pp. 68-77, Mar. 2016.

[8] W. Hao, Y.J. Lin, and X.F. Yang, “Signal progression model for long arterial: intersection grouping and coordination,” *IEEE Access,* vol. 6, pp. 30128-30136, Jun. 2018.

[9] K. Gao, F. Han, P. Dong, N. Xiong, R.Du. Connected vehicle as a mobile sensor for real time queue length at signalized intersections. *Sensors*, vol. 19, no. 9, pp. 2059-2080. May. 2019

[10] C. Ma, W. Hao, A. Wang, and H. Zhao. “Developing a coordinated signal control system for urban ring road under the vehicle-infrastructure connected environment,” *IEEE Access,* vol.6, pp. 52471 - 52478, Sep. 2018.

[11] Y. Li, W. Chen, S. Peeta and Y. Wang, “Platoon control of connected multi-vehicle systems under v2x communications: design and experiments,” *IEEE Trans. Intell. Transp. Syst.,* to be published. DOI: 10.1109/TITS.2019.2905039.

[12] Y. Li, L. Zhang, H. Zheng, X. He, S. Peeta, T. Zheng, and Y. Li, “Nonlane-discipline-based car-following model for electric vehicles in transportation-cyber-physical systems,” *IEEE Trans. Intell. Transp. Syst*., vol.19, no. 1, pp. 38-47, Apr. 2017.

[13] R. V. Haaren, “Assessment of electric cars range requirements and usage patterns based on driving behavior recorded in the National Household Travel Survey of 2009,” *New York, NY, USA: Columbia Univ*., Jul. 2011.

[14] Y. Li, D. Sun, W. Liu, M. Zhang, M. Zhao, X. Liao and L. Tang, “Modeling and simulation for microscopic traffic flow based on multiple headway, velocity and acceleration difference,” *Nonlinear Dyn.*, vol. 60, no. 1-2, pp.15-28, Dec. 2010.

[15] R. Jiang, Q. Wu, and Z. Zhu, “Full velocity difference model for a car-following theory,” *Phys. Rev. E,* vol. 64, no. 1, pp. 017101–017105, Aug. 2001.

[16] Y. Li, L. Zhang, S. Peeta, X. He, T. Zheng, and Y. Li, “A car-following model considering the effect of electronic throttle opening angle under connected environment,” *Nonlinear Dyn.*, vol. 85, pp.2115-2125, May. 2016.

[17] S. Jin, D.H. Wang, X.R. Yang, “Non-lane-based car-following model with visual angle information,” *Transp. Res. Rec*. vol. 2249, no. 1 pp.7-114, Mar. 2011.

[18] Y. Li, H. Zhao, L. Zhang, C. Zhang, “An extended car-following model incorporating the effects of lateral gap and gradient,” *Physica A*, vol. 503, pp.177-189, Mar. 2018.

[19] J.I. Ge, and G. Orosz, “Optimal control of connected vehicle systems with communication delay and driver reaction time,” *IEEE Trans. Intell. Transp. Syst.*, vol.18, no. 5, pp. 2056-2070, Dec. 2016.

[20] L. Li, and X. Chen, “Vehicle headway modeling and its inferences in macroscopic/microscopic traffic flow theory: a survey,” *Transp. Res. Part C: Emerg. Technol.*, vol. 76, pp. 170-188, Mar. 2017.

[21] S. Gong, J. Shen, and L. Du, “Constrained optimization and distributed computation based car following control of a connected and autonomous vehicle platoon,” *Transp. Res. Part B: Methodol,* vol.94, pp. 314-334, Dec. 2016.

[22] J.I. Ge, and G. Orosz, “Dynamics of connected vehicle systems with delayed acceleration feedback,” *Transp. Res. Part C: Emerg. Technol.*, vol.46, pp. 46-64, Sept. 2014.

[23] D. Jia, and D. Ngoduy, “Enhanced cooperative car-following traffic model with the combination of V2V and V2I communication,” *Transp. Res. Part B: Methodol*, vol.90, pp. 172-191, Mar. 2016.

[24] Y. Zheng, S.E. Li, J. Wang, D. Cao, and K. Li, “Stability and scalability of homogeneous vehicular platoon: study on the influence of information

flow topologies," *IEEE Trans. Intell. Transp. Syst.*, vol. 17, no. 1, pp. 14-26, Mar. 2015.
[25] A. Salvi, S. Santini, and A.S. Valente, "Design, analysis and performance evaluation of a third order distributed protocol for platooning in the presence of time-varying delays and switching topologies," *Transp. Res. Part C: Emerg. Technol.*, vol. 80, pp. 360-383, Apr. 2017.
[26] Y. Li, C. Tang, K. Li, S. Peeta, X. He, and Y. Wang, "Nonlinear finite-time consensus based connected vehicle platoon control under fixed and the switching communication topologies," *Transp. Res. Part C: Emerg. Technol.*, vol. 93, pp. 525-543, Jun. 2018.
[27] X. Wu, X. He, G. Yu, A. Harmandayan, and Y. Wang, "Energy-optimal speed control for electric vehicles on signalized arterials," *IEEE Trans. Intell. Transp. Syst.*, vol. 16, no. 5, pp. 2786-2796, Apr. 2015.
[28] S. Thrun, M. Montemerlo, H. Dahlkamp, D. Stavens, A. Aron, J. Diebel, et al., "Stanley: the robot that won the darpa grand challenge," *J. Field Robot*, vol. 23, No. 9, pp. 661-692, Jun. 2006.
[29] C. Urmson, J. Anhalt, D. Bagnell, C. Baker, R. Bittner, M.N. Clark, et al., "Autonomous driving in urban environments: boss and the urban challenge," *J. Field Robot*, vol. 25, No. 8, pp. 425-466, Jan. 2008.
[30] Y. Li, C. Tang, S. Peeta, and Y. Wang, "Nonlinear consensus based connected vehicle platoon control incorporating car-following interactions and heterogeneous time delays," *IEEE Trans. Intell. Transp. Syst.*, vol. 20, no. 6, pp. 2209-2219, May. 2019.
[31] J. Monteil, R. Billot, J. Sau, and N.E.E. Faouzi, "Linear and weakly nonlinear stability analyses of cooperative car-following models," *IEEE Trans. Intell. Transp. Syst.*, vol. 15, no. 5, pp. 2001-2013, May. 2014.
[32] K. C. Dey, A. Rayamajhi, M. Chowdhury, P. Bhavsar, and J. Martin, "Vehicle-to-vehicle (V2V) and vehicle-to-infrastructure (V2I) communication in a heterogeneous wireless network—performance evaluation," *Transp. Res. Part C: Emerg. Technol.*, vol. 68, pp. 168-184, Jul. 2016.
[33] C. Campolo, A. Vinel, A. Molinaro, and Y. Koucheryavy, "Modeling broadcasting in IEEE 802.11p/WAVE vehicular networks," *IEEE Commun. Lett.*, vol. 15, no. 2, pp. 199–201, Feb. 2011.

Hang Zhao received his M.S. degree in control science and engineering with Chongqing University of Posts and Telecommunications, Chongqing, China, in 2019.

He is currently working toward the Ph. D degree in control science and engineering with Chongqing University, Chongqing, China. His research interests include traffic flow modeling and connected vehicles.

Yongfu Li (M'16) received the Ph. D degree in control science and engineering from Chongqing University, Chongqing, China, in 2012.

He is currently a Full Professor of control science and engineering and Director of Key Laboratory of Intelligent Air-Ground Cooperative Control for Universities in Chongqing. His research interests include connected and automated vehicles, intelligent transportation systems, and cooperative control theory and application.

Wei Hao received his Ph.D. degree in civil engineering from New Jersey Institute of Technology, USA, in 2013.

He is currently a Professor of Changsha University of Science and Technology in China. His areas of expertise include traffic operations, ITS, planning for operations, traffic modeling and simulation, connected automated vehicles, and travel demand forecasting.

Srinivas Peeta received the Ph. D degree in civil engineering from University of Texas at Austin, U.S.A., in 1994.

He is the Frederick R. Dickerson Chair and Professor in the Schools of Civil and Environmental Engineering and Industrial and Systems Engineering at Georgia Institute of Technology. He is also Principal Research Faculty at the Georgia Tech Research Institute. His research interests include intelligent transportation systems (ITS), operations research, control theory, and computational intelligence techniques.

Yibing Wang (M'03) received the Ph.D. degree in control theory and applications from Tsinghua University, Beijing, China, in 1998.

He is currently a Full Professor with the Institute of Transportation Engineering, the College of Civil Engineering and Architecture, Zhejiang University, Hangzhou, China. His research interests include traffic flow modeling, freeway traffic surveillance, ramp metering, route guidance, urban traffic signal control, and vehicular ad hoc networks.